PAPER

Check for updates

The effect of precipitation on gaseous oxidized and elemental mercury concentrations as quantified by two types of atmospheric mercury measurement systems

Peter S. Weiss-Penzias, [ID] *[a] Seth N. Lyman,[bc] Tyler Elgiar,[b] Lynne E. Gratz,[d] Winston T. Luke,[e] Gabriel Quevedo,[f] Nicole Choma[g] and Mae Sexauer Gustin[g]

Gaseous and particulate-bound oxidized mercury (Hg) compounds (Hg^{II}) have high solubility in precipitation compared to gaseous elemental Hg (Hg^0). Wet and dry deposition are the primary routes of entry for atmospheric Hg^{II} into aquatic ecosystems. Information on how much Hg^{II} is removed from the atmosphere to the landscape during precipitation is lacking. In this study, oxidized Hg^{II} concentrations were measured with a dual-channel system (DCS) at two sites in the United States, Storm Peak Laboratory (SPL), in Colorado (2021–2022), and Beltsville (MD99) in Maryland (2022–2024), and compared with data from 16 co-located Atmospheric Mercury Network (AMNet) and Mercury Deposition Network (MDN) sites that used a KCl denuder method. At the two DCS sites, gaseous oxidized Hg concentrations were segregated by wet and dry periods from the nearest precipitation gauge to determine values for median dry Hg^{II} and median wet Hg^{II} concentrations (dry-wet = "Hg^{II}" washout") for each site. SPL had higher median ambient Hg^{II} and higher median Hg^{II} washout (90 pg m^{-3} and 22 pg m^{-3}, respectively) compared to that for MD99 (43 pg m^{-3} and 7 pg m^{-3}). This difference could be due to site elevation (3161 *vs.* 77 m) as there is generally more Hg^{II} higher in the atmosphere. In contrast, the ambient Hg^{II}/washout Hg^{II} ratios were more similar, 4.1 for SPL and 5.8 at MD99. The mean ambient Hg^{II}/washout Hg^{II} ratio for the 16 AMNet sites was 1.8 ± 0.1. The AMNet Hg^{II} data are known to be biased low due to issues with the KCl-denuder method, and this low bias appears to result in lower ambient Hg^{II}/washout Hg^{II} ratio observed for the AMNet sites. Correction factors for AMNet data using Hg^{II} measurements from DCS instruments were found to range from 2–3 and could be used to improve the accuracy of older data.

Environmental significance

Oxidized mercury (Hg) compounds in the atmosphere, both in gaseous and particulate forms, are the main sources of Hg in precipitation, which contributes Hg to aquatic ecosystems where it is transformed into methylmercury. Understanding the connection between emissions of Hg to the atmosphere and their contribution to Hg in precipitation is limited by several factors including uncertainties associated with the measurement methods for oxidized Hg. In this study, an improved measurement method for oxidized Hg was utilized at a mountaintop site in the Rocky Mountains and at a suburban site in Maryland, where high-resolution datasets were obtained at each site for two-year periods. The data were separated by precipitation depth as measured by the closest rain gauge (>0 (wet) and =0 (dry)). The medians of each of these categories were calculated and median wet-median dry was then termed oxidized Hg "washout". We then calculated the ratio of ambient oxidized Hg to washout oxidized Hg and found the ratios to be relatively consistent at the two sites that used the improved instrumental method. The mean ratio for these two sites was then used to correct older measurements of oxidized Hg across a network of 16 sites in the U.S. and Canada, which had a mean ratio of ambient oxidized Hg to washout oxidized Hg that was 2.7 times lower. This analysis revealed that the older oxidized Hg data could be adjusted upward by factors of 2–3 depending on the site. We suggest that assessments of the impact of Hg emissions on Hg in precipitation could be underestimated if only uncorrected data were used.

[a]University of California, Santa Cruz, Santa Cruz, CA 95064, USA. E-mail: pweiss@ucsc.edu

[b]Bingham Research Center, Utah State University, Vernal, UT, USA

[c]Department of Chemistry and Biochemistry, Utah State University, Logan, UT, USA

[d]Department of Chemistry and Environmental Studies Program, Reed College, Portland, OR, 97202, USA

[e]Air Resources Laboratory, National Oceanic and Atmospheric Administration, College Park, Maryland 20740, USA

[f]University of California, Los Angeles, Los Angeles, CA, USA

[g]University of Nevada, Reno, Reno, NV, USA

© 2025 The Author(s). Published by the Royal Society of Chemistry

1 Introduction

Mercury (Hg) is a global toxicant that affects humans and wildlife through the dietary intake of methylmercury,[1,2] as evidenced by recent Hg concentration surveys of high trophic level and sentinel species that showed exceedances of benchmarks for fish and wildlife.[3] Most Hg pollution is emitted to the atmosphere, where it is transported and transformed from the relatively inert elemental form (Hg^0) to the divalent form (Hg^{II}) that is more reactive and water-soluble.[4] Experimental, theoretical, and modeling advances have suggested that Hg^0 is initially oxidized by Br and OH, and subsequently by ozone and other atmospheric constituents,[5] and much of the resultant gas-phase Hg^{II} subsequently becomes part of dissolved organic compound complexes in aerosols and cloud droplets.[6] Gas- and aerosol-phase Hg^{II} can then either be photochemically reduced back to Hg^0 or wet and dry deposited to the Earth's surface.[7–10] Other atmospheric Hg redox pathways may also exist; however, understanding of atmospheric Hg chemistry is currently hindered by an inability to identify specific Hg^{II} compounds in the atmosphere. Hg^0 can also be dry deposited to terrestrial vegetation through stomatal uptake, and by some estimates this is the dominant removal pathway,[11] although bidirectional exchange releases Hg back to the atmosphere from plants and soil surfaces.[12,13]

Wet deposition of Hg is measured by collection of precipitation that contains particulate and soluble forms of Hg^{II}. Wet deposition is an important source of Hg to ecosystems where Hg^{II} undergoes methylation by microbes and enters the food web.[14] However, controls on methylmercury formation and concentrations in the environment are numerous, and there is not a simple relationship between wet deposition of inorganic Hg and methylmercury in fish.[15] Although atmospheric washout as a removal phenomenon for Hg was identified years ago through observations of the decrease in Hg concentrations in sequential rain samples,[16,17] the origins of Hg^{II} in precipitation are not well known. One complicating factor is that most measurements of ambient Hg^{II} concentrations have been collected using methods that are now known to be biased low due to interferences on the KCl-denuder and the quartz fiber filter.[18,19] A second factor is that most wet deposition measurements made by the Mercury Deposition Network (MDN) that is part of the National Atmospheric Deposition Program (NADP) are weekly samples limiting the ability to quantitatively determine Hg^{II} sources using individual precipitation events.

There is considerable evidence that rainfall has a diluting effect on Hg concentrations in precipitation ($[Hg]_{aq}$) and that a log–log relationship exists between $[Hg]_{aq}$ and precipitation depth both in weekly integrated and event-based samples.[20–27] Scavenging coefficients of Hg in precipitation are lower than for other airborne metals and ions due to a continuous supply of soluble forms of Hg^{II} at least in the vicinity anthropogenic emissions.[21] Gaseous oxidized Hg (GOM) is generally more water soluble than particulate bound Hg (PBM) and is thought to contribute more to $[Hg]_{aq}$ than PBM,[21] although the opposite could occur in polluted urban atmospheres with heavy burdens of particulate matter.[27] Some studies have suggested that Hg^{II} is incorporated into precipitation via gas-phase inclusion or particulate nucleation within the cloud, with below-cloud scavenging in the boundary layer probably being less important.[21,28] Indeed, Shah and Jaeglé,[29] in a modeling study, found that Hg^{II} produced in the upper and middle troposphere constitutes 91% of the annual Hg^{II} wet deposition flux. This may be specifically true in the western U.S. where the free troposphere is an important source of surface GOM and PBM, and wet deposition of Hg increases with altitude.[30,31]

Because of the importance of Hg wet deposition to ecosystems, monitoring networks have been established to make regular, standardized measurements of Hg loads to surfaces. The MDN is currently composed of 76 active sites that collect weekly precipitation samples to be analyzed for $[Hg]_{aq}$.[32] At 16 MDN sites, there were measurements of atmospheric speciated Hg concentrations (PBM, GOM, and Hg^0) carried out for multiyear periods by AMNet during the years 2008–2020. Although these atmospheric Hg data sets are large and potentially valuable for understanding the origins of Hg in wet deposition, the quantitative accuracy of these data is in question because PBM and GOM measurements are subject to low-bias and interferences, due to the use of the KCl denuder and quartz filter, respectively.[10,33,34] In response, alternative techniques have been developed that quantify Hg^{II} compounds using cation-exchange membranes in dual-channel systems that can measure Hg^{II} by difference (total Hg–Hg^0),[35–39] but datasets are from fewer locations and do not span as much time as the AMNet data.

Prior to the understanding of the limitations of the KCl-denuder based measurements, comparisons were made using the 2–3 h GOM and PBM concentrations with weekly $[Hg]_{aq}$ at co-located sites in AMNet/MDN[40] to make predictions of GOM + PBM concentrations at MDN-only sites. Later, Cheng et al.[41] made use of PBM measurements from AMNet sites and scavenging ratios of major ions in wet deposition from measurements at MDN sites to estimate the proportion of GOM, and coarse and fine PBM in precipitation. These scavenging ratios[42] were then combined with weekly GOM concentrations from AMNet to estimate measurement biases of the KCl-denuder measurement system which ranged from 1.3–14.3 (mean = 2.3) times below predicted values. This range is similar to that suggested by Gustin et al.[43] (1.6–12) and Gustin et al.[44] (1.3–13), both of which were based on comparison between measurements by different methods.

Using uncorrected Hg^{II} concentration data taken with the KCl-denuder method could therefore be leading to misinterpretations regarding the relationship between Hg^{II} concentrations in air and $[Hg]_{aq}$ that is measured at an MDN site, resulting in uncertainties about the source of Hg^{II} in precipitation. For example, Lynam et al.[45] saw Hg rainfall concentrations 2–4 times higher for concurrent events with similar precipitation depth at an urban site compared to a background site suggesting that scavenging of local Hg emissions was occurring. On the other hand, away from location emission sources, there may be a weak relationship between ambient Hg^{II} and $[Hg]_{aq}$. A model evaluation study at the global level showed a variation of only ±10% in wet deposition for three different Hg emissions scenarios.[46] Similarly, simulated Hg wet deposition flux in New York State changed only by 2% despite a near doubling of emissions in the Northeastern U.S.[25] Considering the importance of the middle and upper troposphere as a source region for Hg^{II} in wet

© 2025 The Author(s). Published by the Royal Society of Chemistry

Environ. Sci.: Atmos., 2025, **5**, 204–219 | **205**

deposition,[29] changes in surface concentrations of Hg^{II} may not be correlated with $[Hg]_{aq}$ in many locations.

In the current study, the effects of precipitation on air concentrations of Hg^{II} and Hg^0 as measured with the dual-channel systems, which have been shown to quantitatively recover $HgBr_2$ and $HgCl_2$, at a remote high elevation site in the Rocky Mountains and in suburban Maryland were studied. The magnitudes of Hg^{II} washout (median $[Hg^{II}]_{dry}$–median $[Hg^{II}]_{wet}$) and Hg^0 enhancement (median $[Hg^0]_{wet}$–median $[Hg^0]_{dry}$) were quantified at these sites over multiple years of data and seasonal patterns, and air mass histories were examined. It was then considered whether the information learned about precipitation-driven changes in Hg^{II} and Hg^0 species from the dual-channel systems could be used to correct for biases in the AMNet GOM and PBM data (obtained with KCl-denuder/quartz filter measurement system) from 16 co-located AMNet-MDN sites. The mean DCS-derived ambient Hg^{II}/ washout Hg^{II} ratio was determined and the subsequent analyses explored whether this ratio could be used as a correction of older measurement data from 16 co-located sites.

2 Methodology

2.1 Dual-channel measurement sites

2.1.1 Storm Peak Laboratory. Storm Peak Laboratory (SPL) is in the Park Range, a subrange of the Rocky Mountains in northwestern Colorado in the U.S. (40.452254°N and 106.749542°W, 3161 meters above sea level (A.S.L.)).[47,48] Hg^{II} and Hg^0 measurements were made between March 12–October 11, 2021, and again from March 3–September 22, 2022.

Elemental and total gaseous Hg were measured in ambient air at SPL using the dual-channel system.[49–51] The system sampled air at 9 L min^{-1} through a PTFE-coated, heated (120 °C) elutriator and impactor that removed particles larger than 2.5 μm, through 0.5 m of heated perfluoroalkoxy (PFA) Teflon line, and then into one of two channels. One channel included a 650 °C thermolyzer to convert all atmospheric Hg to Hg^0, measuring total atmospheric Hg, and the other a series of two cation-exchange membranes that retain Hg^{II}, to measure only Hg^0. A Tekran 2537X analyzer customized to reduce the sample line volume and to increase sensitivity quantified the Hg^0 output from both channels via the peak height method (cf. ref. 52), and Hg^{II} was calculated as the difference between the two channels. Poly(tetrafluoroethylene) (PTFE) Teflon valves were used to switch air sampled between the two channels at 5 min intervals. The instrument had a 1 h detection limit for Hg^{II} of less than 12 pg m^{-3} ($3\times$ standard deviation of ambient air measurements) and an expanded measurement uncertainty of 16%. Hg^{II} concentrations in this paper are reported to the ones place with no digit after the decimal point. The dual-channel system has been shown to quantitatively collect gas-phase Hg^{II} compounds and Hg^0 injected into ambient air from an SI-traceable calibration source.[42,50] Cation-exchange membranes used in the system to capture Hg^{II} have been shown to collect a wide variety of Hg^{II} compounds and do not collect a significant amount of Hg^0.[53] While no calibration method exists for particle-phase Hg, it is assumed that the dual-channel system captures all gas-phase Hg^{II} and Hg^{II} bound to

particles smaller than 2.5 μm. Information about earlier versions of the dual-channel system and calibrator is available in Lyman et al.[37] and Dunham-Cheatham et al.[50] Soda lime traps were upstream of the 2537X to scrub reactive gases that can passivate the gold traps in the instrument. Soda lime traps and cation-exchange membranes were replaced biweekly. Periodic injections of Hg^0 from a temperature controlled saturated Hg^0 vapor source resulted in recovery of $101 \pm 6\%$.

2.1.2 Beltsville, MD (MD99). The National Oceanic and Atmospheric Administration (NOAA)'s Beltsville site is near Beltsville, Maryland (39.0284N, 76.8172W, 77 m amsl), on the campus of the United States Department of Agriculture's Beltsville Agricultural Research Center and bordering the U.S. Fish and Wildlife Service's Patuxent National Wildlife Refuge (NWR). It is one of the National Atmospheric Deposition Program (NADP)'s Atmospheric Mercury Network (AMNet) sites (site ID: MD99).[54] MD99 is also an MDN site, thus unlike Storm Peak Laboratory, there was no geographic separation between the atmospheric measurements and precipitation collection. A 10 m walk-up tower was established in a clearing surrounded by grassland and forest. All chemical analyzers are housed in a climate-controlled shelter adjacent to the tower. Ongoing measurements of atmospheric Hg species are made from the top of the tower with an inlet height of 10.6 m above ground to minimize local surface effects.

Oxidized mercury measured at MD99 as the difference between total Hg (THg) and gaseous elemental Hg. A Tekran® 1135 Particulate Unit module was modified to serve as the NOAA difference system. A custom pyrolyzer (URG Corp., Chapel Hill, NC) was based on a modified design of the Tekran® Corp. Regenerable Particle Filter (RPF). A porous quartz frit was fused approximately 5 cm from the threaded inlet of the pyrolyzer to minimize inlet losses of Reactive Mercury (RM) species and supported a 22 mm diameter quartz fiber filter and quartz wool plug. Quartz chips were packed behind the quartz frit to pyrolyze all mercury species to Hg^0 at 800 °C. The pyrolyzer inlet was typically filtered with a PTFE membrane (25 mm diameter, 1 μm pore size) that was assumed to capture particle-phase Hg^{II} and allow gas-phase Hg^{II} to pass through.

Gaseous elemental Hg was measured by pulling air through two 47 mm diameter polyether sulfone (PES) membranes (0.22-micron pore size, MilliporeSigma™ Express™ PLUS Membrane Filters) to remove all PBM and GOM. We note that, while Dunham-Cheatham et al.[55] found no significant difference between the cation-exchange membranes used at Storm Peak and the PES membranes used at Beltsville, Allen et al.[56] found that PES membranes captured 14–23% less Hg^{II} than cation-exchange membranes (which are PES that have been treated with a proprietary process). The filters were housed in a Sulfinert (Restek, Bellafonte, PA) coated open-faced stainless steel filter holder (Model FJ-42SS, F&J Specialty Products, Inc., Ocala FL). The filters and holder were thermostatically controlled at 40 °C and were situated along the bottom edge of the 1135 module. All inlet filters were changed monthly, and the pyrolyzer was cleaned and replaced quarterly. Soda lime traps upstream of each 2537X analyzer were changed weekly. Ambient air was sampled through each channel at 1.0 standard liters per minute (0 °C, 1 atm), controlled by the Tekran analyzers.

The Tekran 1135 inlet module was mounted atop the 10 m walk-up scaffold at MD99. Two 50-foot lengths of $\frac{1''}{4}$ diameter PFA Teflon tubes, encased in an insulated umbilical (Thermon Manufacturing) maintained at 50 °C, routed the flows from the THg and Hg⁰ channels to a valve switching box containing a series of PFA Teflon valves in the instrument shelter below. The valve switching assembly was connected to two Tekran® 2537X analyzers, and a Labview program actuated the valves to allow both analyzers to independently measure both THg and Hg⁰. The analyzers operated asynchronously, so that when analyzer 1 (X1) measured THg, Analyzer 2 (X2) measured Hg⁰, and *vice versa*. Each channel was sampled for two 6 minutes cycles by each analyzer. Hg^{II} was calculated as the difference of the hourly-averaged THg and Hg⁰ concentrations for each analyzer. The limit of detection was estimated as ±2 standard deviations of the average difference when the pyrolyzer was operated at 50 °C. LODs of 10–15 pg m^{-3} were achieved.

2.2 AMNet and MDN data

Measurements of atmospheric PBM, GOM, and Hg⁰ have been made at 22 AMNet sites that also collect weekly precipitation samples analyzed for [Hg]$_{aq}$ concentration (MDN sites). Of these, 16 had sufficient data coverage to warrant detailed analysis (>1 year) (Fig. 1). Summary data for Hg concentrations measured at these sites is shown in Appendix A. Based on geography, and monthly and diel concentrations of Hg forms (Appendix A, Table 4) the AMNet sites were grouped into four categories: Local Emissions (AL19, IN21, NY06, NY43, OH02, UT97), Suburban North (MD08, MD99, NJ30, WI07), Suburban South (FL96, GA40, MS12, OK99), and Rural North (NS01, VT99).

Concentrations of the different forms of mercury in the AMNet network were quantified by automated Tekran® 1130/1135/2537 systems.[57] All instrumentation across each site was operated in an identical manner according to standard operating procedures provided by AMNet. The Tekran® 1135 measures PBM <2.5 μm. GOM and PBM concentrations were determined every 3 h with 1–2 h sampling and 1 h desorption times. Hg⁰ was sampled and analyzed every 5 minutes and combined into hourly averages in the raw AMNet data set. AMNet GOM and PBM concentrations in this paper are reported to the ones place with no digits after the decimal point. Mercury concentrations in precipitation samples taken at the AMNet/MDN co-located sites were measured according to standardized protocols.[32] Only validated data were used for this analysis. In this paper, Hg^{II} and Hg⁰ are used to refer to oxidized and elemental mercury measurements made at SPL and MD99 with the dual-channel system, whereas GOM, PBM, and Hg⁰ refer to the Hg forms measured using the Tekran® 1130/1135/2537 system, respectively.

2.3 Data analysis

Data tables from each site were used in their original downloaded formats to determine when there was precipitation at each site and to classify the Hg measurements accordingly. Hourly precipitation depth data reported by the electronic rain gauge associated with the MDN sites were used to classify individual Hg measurements at all sites as "wet" (precipitation depth >0) or "dry" (precipitation depth =0). Median concentrations for all Hg forms during "wet" or "dry" periods were calculated and used for subsequent comparisons between sites and between measurement systems. Using median wet and median dry concentrations, Hg^{II} washout for a given site over its record of measurement was defined as

$$[Hg^{II}]_{washout} = [Hg^{II}]_{dry} - [Hg^{II}]_{wet} \qquad (1)$$

Medians were selected instead of means because of the large number of high concentrations of Hg^{II} in the AMNet, SPL, and
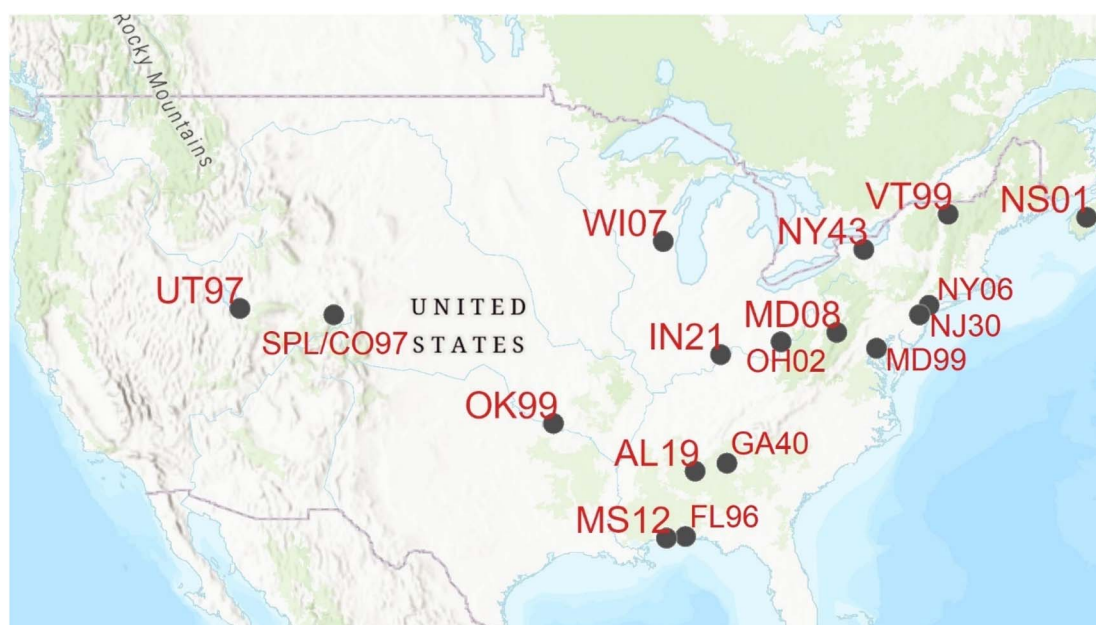

Fig. 1 Map showing the co-located AMNet and MDN sites in the U.S. and Canada and the SPL site which was paired with MDN-only site CO97.

© 2025 The Author(s). Published by the Royal Society of Chemistry

Environ. Sci.: Atmos., 2025, **5**, 204–219 | **207**

MD99 datasets that greatly skewed the means but not the medians. When normally distributed datasets are grouped, means are reported. For the AMNet data, $[GOM]_{washout}$ and $[PBM]_{washout}$ were calculated separately and then combined to determine Hg^{II} washout:

$$[Hg^{II}]_{washout} = [GOM]_{washout} + [PBM]_{washout} \quad (2)$$

The ratio of median ambient Hg^{II} concentration to the median Hg^{II} washout concentration was calculated for each site. A correction factor for ambient Hg^{II} concentrations measured at the AMNet sites was calculated using

$$[Hg^{II}]_{correction,AMNet} = \frac{\left[Hg^{II}_{ambient,REF}\right]}{\left[Hg^{II}_{washout,REF}\right]} \Big/ \frac{\left[Hg^{II}_{ambient,AMNet}\right]}{\left[Hg^{II}_{washout,AMNet}\right]} \quad (3)$$

where REF refers to the reference data, that being the mean ratios from the DCS sites.

For Hg^0 a precipitation enhancement was calculated

$$[Hg^0]_{enhancement} = [Hg^0]_{wet} - [Hg^0]_{dry} \quad (4)$$

Relationships between the Hg concentration in weekly integrated precipitation samples ($[Hg]_{aq}$) and the air concentrations of Hg forms along with values of other ancillary meteorological and chemical parameters were also investigated. At SPL and MD99, a weekly $[Hg]_{aq}$ was compared with mean values of chemical and meteorological parameters by selecting those parameters' values that corresponded to when precipitation depth >0 and neglecting values when precipitation depth =0. For the MDN sites weekly $[Hg]_{aq}$ was compared against GOM + PBM = Hg^{II} concentrations averaged over the same weekly time step as the MDN sample, which included both dry and wet precipitation states.

AMNet data were further reduced to monthly and hourly means to characterize the seasonal and diel cycles (Appendix A, Fig. 8 and 9).

Statistical analyses included one-way ANOVA tests, linear regressions, multiple linear regressions, principal component analyses, and Shapiro–Wilk and Kolmogorov–Smirnov normality tests. OriginPro 2021 (OriginLab) was used for these tests. Statistical significance was met if the test statistic was <0.05. Hg^{II} concentrations were not normally distributed for any of the sites (except for SPL) therefore log transformation was carried out before further analysis.

2.4 Other chemical and meteorological measurements at SPL

Meteorological data were collected on the roof of SPL at a height of 10 m above ground level (AGL) at five-minute time resolution.[51] Ozone (O_3) was measured at a time resolution of 1 minute and calibrated daily using a Thermo Model 49i Analyzer with a precision of 1.0 ppb. As no precipitation data was collected at SPL, this study relied upon hourly precipitation measurements over the measurement period at SPL from the MDN site CO97 at Buffalo Pass, located 9 km to the northwest from SPL in the same mountain range at an elevation of 3234 m A.S.L. More details on the SPL ancillary measurements are given in Derry et al.[51]

Back trajectory simulations for SPL were performed using the NOAA Air Resources Laboratory GDAS 1° data archive and Hybrid Single-Particle Lagrangian Integrated Trajectory (HYSPLIT) (http://ready.arl.noaa.gov/HYSPLIT.php) for the timespan March 12–September 30, 2021. Back trajectories were initialized every six hours for starting locations in a 0.5° × 0.5° grid centered on SPL. The initial trajectory heights were 100, 300, and 500 m above the ground, and the trajectories went backward 24 hours. Each trajectory contains information on the modeled boundary layer height, and this was used to calculate the mean height of the multiple trajectories above the boundary layer. All initial trajectory locations and heights were reduced to a 6 h average (mean of $N = 675$ trajectories). The mean pressure of the trajectories at time = 0 for a subset between the dates May 1–June 14, 2021, was 704 mbar (averaging all the 100, 300, and 500 m AGL starting heights) that is similar to the mean barometric pressure (698 mbar) during the previous study.[47] This indicates that while the

Table 1 Summary statistics of Hg^{II} and Hg^0 concentrations measured with the dual-channel system, segregated into wet and dry categories and the difference between these two categories (dry-wet for Hg^{II} and wet-dry for Hg^0)

Site	Parameter (unit)	N (hourly)	Mean	Median	Std dev.	SE
SPL	Hg^{II} all (pg m^{-3})	7469	93	90	43	0.5
SPL	Hg^{II} wet (pg m^{-3})	703	71	70	34	1.3
SPL	Hg^{II} dry (pg m^{-3})	6766	96	92	43	0.5
SPL	Hg^{II} dry-wet (pg m^{-3})		25	22	9	0.3
SPL	Hg^0 all (ng m^{-3})	7574	1.256	1.270	0.118	0.001
SPL	Hg^0 wet (ng m^{-3})	722	1.301	1.314	0.094	0.004
SPL	Hg^0 dry (ng m^{-3})	6944	1.250	1.264	0.117	0.001
SPL	Hg^0 wet-dry (ng m^{-3})		0.051	0.050	0.033	0.020
MD99	Hg^{II} all (pg m^{-3})	10 465	44	43	23	0.2
MD99	Hg^{II} wet (pg m^{-3})	699	37	36.6	16	0.2
MD99	Hg^{II} dry (pg m^{-3})	9766	45	44.0	23	0.6
MD99	Hg^{II} dry-wet (pg m^{-3})		8	7	7	0.3
MD99	Hg^0 all (ng m^{-3})	14 186	1.288	1.289	0.150	0.001
MD99	Hg^0 wet (ng m^{-3})	846	1.341	1.347	0.135	0.001
MD99	Hg^0 dry (ng m^{-3})	12 414	1.289	1.297	0.143	0.005
MD99	Hg^0 wet-dry (ng m^{-3})		0.052	0.050	0.008	0.004

terrain at SPL is complex and meteorological fields are coarse, the back trajectory starting points reasonably represented the surface. For the comparison of $[Hg]_{aq}$ with mean back trajectory height, back trajectory data representing wet conditions were selected 12 h before the onset of precipitation at CO97 until the end time of the precipitation. This data selection decision was made to boost the number of 6 h observations used for averaging, since precipitation events were sometimes only a few hours per week, and to get a representation of the atmosphere just before the precipitation event. If two precipitation events were separated by 24 h or less in time, then an unbroken record of the 6 h data was selected until the end of the precipitation event.

3   Results and discussion

3.1   Storm Peak Lab and CO97 Hg data

Hg^{II} and Hg^0 concentrations measured at Storm Peak Lab with the Dual-Channel System during March–October 2021 and March–September in 2022 (ref. 51) were aligned with hourly precipitation measurements from Buffalo Pass (CO97). Table 1 shows the mean and median values for Hg^{II} and Hg^0 grouped by precipitation state (dry or wet). Hg^{II} concentrations were statistically significantly lower during wet periods with a difference between the medians of each group of 22 pg m^{-3} (Fig. 2a). Hg^{II} measurements classified as wet constituted 9.4% of the total measurements. Hg^{II} was washed out of the atmosphere during precipitation, however Hg^0 was released as shown by a wet-dry difference in median Hg^0 concentrations of 0.052 ng m^{-3}, equivalent to a 4.2% increase (Fig. 2b). The effect of season on Hg^{II} washout and Hg^0 enhancement is shown in Fig. 2c and d. Hg^{II} washout can be seen in all months except March, and Hg^0 enhancement occurred in all months except October. Both Hg species displayed little seasonality at SPL.[51]

Hg^{II} and Hg^0 concentrations plus ancillary parameters at SPL were compared with $[Hg]_{aq}$ concentrations in the weekly precipitation sample at CO97 (Table 2). Log$[Hg]_{aq}$ was significantly positively correlated with the following parameters: log Hg^{II}, log sample volume, relative humidity, ozone concentrations, PM10 aerosol scattering, and the mean altitude of 24 h back trajectory heights arriving at SPL (Table 2). Principal component analysis (Appendix A, Fig. 7) showed that the first component was consistent with a relatively strong anti-correlation between $[Hg]_{aq}$ and %RH. Taken together, these
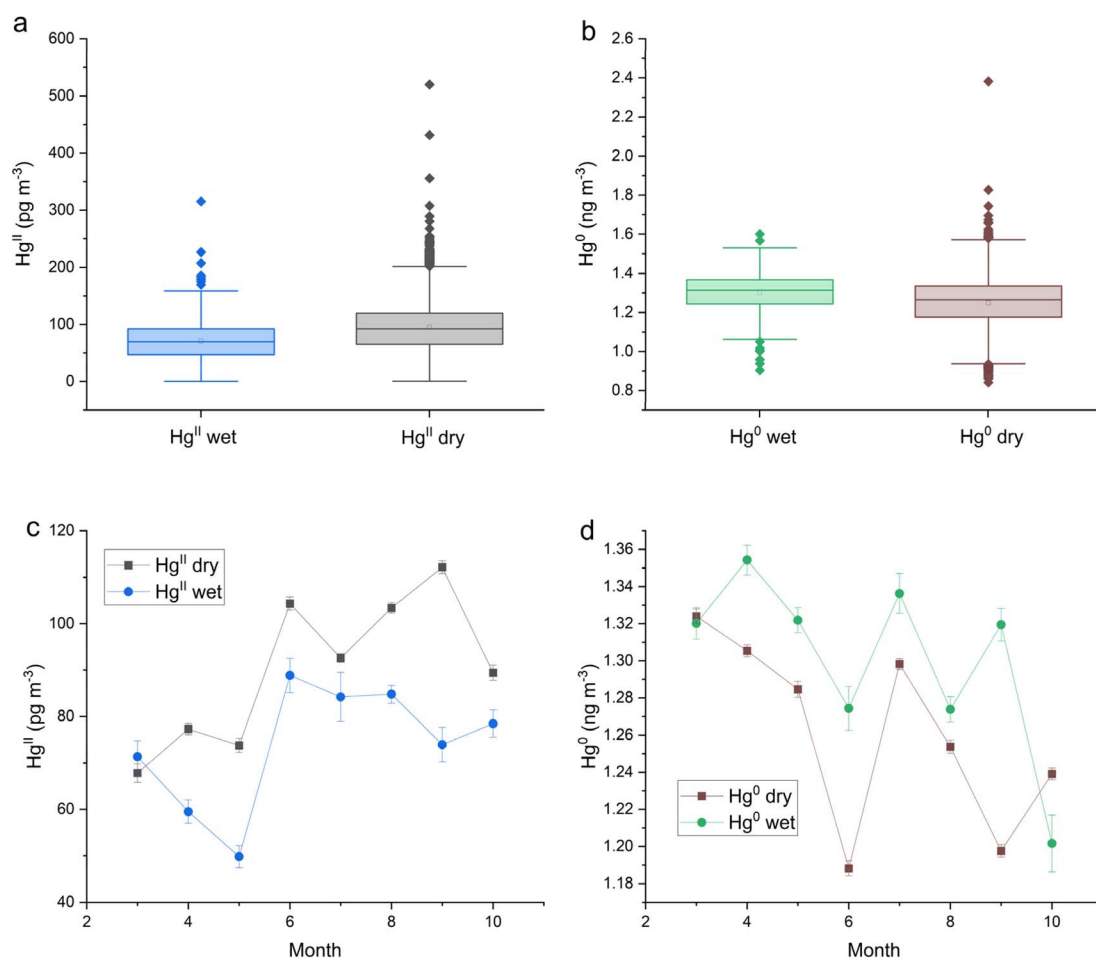

Fig. 2   Storm Peak Laboratory (SPL) box and whisker plots of (a) Hg^{II} and (b) Hg^0 concentrations by precipitation state, and (c) Hg^{II} and (d) Hg^0 monthly medians by precipitation state. These data were measured with a dual-channel measurement system. Error bars in (c) and (d) represent the standard error.

Table 2 Linear correlation coefficients between the MDN weekly sample $[Hg]_{aq}$ concentration and other parameters measured at SPL and MD99. Correlation coefficients in bold are statistically significant

Linear correlation with log $[Hg]_{aq}$	SPL (DCS) r^2	MD99 (DCS) r^2
Log sample volume	−0.02	**0.30**
Hg^0	−0.03	−0.01
Hg^{II}	**0.09**	0.00
O_3	**0.24**	
Log PM10 scattering	**0.33**	
%RH	**0.39**	
Back trajectory height	**0.27**	

relationships suggest that precipitation that originates higher in the troposphere, as indicated by the trajectory heights, higher ozone, and lower relative humidity, generally has higher $[Hg]_{aq}$, which is consistent with the recent analysis by Derry *et al.*,[51] Shah and Jaeglé's[29] model results, and the work of Huang and Gustin.[30] A weak correlation between Hg^{II} measured at SPL with $[Hg]_{aq}$ in a weekly precipitation sample is consistent with the source of Hg^{II} washout at this site being primarily entrainment of middle free tropospheric air into the storm system many days before reaching the site.[51]

3.2 Beltsville, MD (MD99) Hg data

The dual-channel system Hg^{II} and Hg^0 measurements at this site were aligned with hourly precipitation data to determine which measurements were grouped either wet or dry. Like the trend observed at SPL, Hg^{II} concentrations at MD99 were statistically significantly lower during wet periods with the difference between the medians of dry and wet being 7 pg m^{-3} (Table 1 and Fig. 3a). The proportion of Hg^{II} measurements classified as wet was 7.0%. Hg^0 concentrations were significantly higher during wet periods with a significant difference between the medians of 0.049 ng m^{-3} (Table 1 and Fig. 3b). Seasonal effects for both Hg^{II} washout and Hg^0 enhancement are evident in Fig. 3c and d. For Hg^{II}, washout occurred mainly from Feb to July, peaking in the months of April and June. For Hg^0, the months of Jun.–Dec. showed the most enhancement.

Hg^{II} and Hg^0 concentrations at MD99 were compared with $[Hg]_{aq}$ concentrations in each weekly precipitation sample (Table 2). Log$[Hg]_{aq}$ was negatively correlated with log sample volume due to the dilution effect, with the relationship being significant. However, neither Hg^{II} nor Hg^0 showed a significant correlation with log$[Hg]_{aq}$ at MD99. Principal component analysis for MD99 data (Appendix A, Fig. 7) showed that the first component is associated with elevated $[Hg]_{aq}$ and lower sample volume, *i.e.*, the dilution effect.
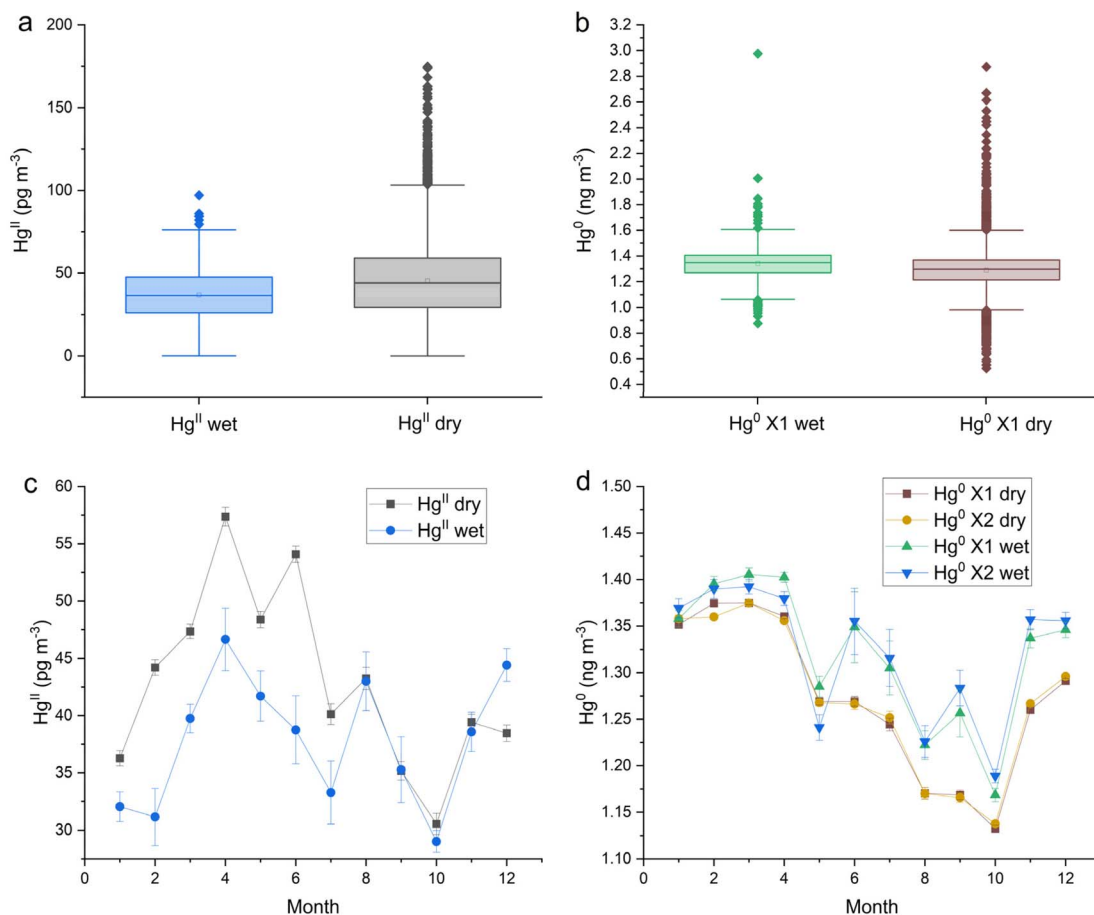

Fig. 3 Beltsville, MD (MD99) box and whisker plots of (a) Hg^{II} and (b) Hg^0 concentrations by precipitation state, and (c) Hg^{II} and (d) Hg^0 monthly medians by precipitation state. These data were measured with a dual-channel measurement system. X1 and X2 refer to two Tekran 2537X instruments used.

3.3   Gaseous and aqueous Hg data from 16 co-located AMNet-MDN sites

Co-located AMNet-MDN sites were categorized based on patterns of mean Hg concentrations in seasonal and diel cycles (in Appendix A, see Table 4, Fig. 8, and 9), and each site was assigned one of four site types: Local Emissions, Suburban North, Suburban South, Rural North. At each site, GOM, PBM, and Hg^0 concentrations were paired with the corresponding hour when precipitation was >0 to produce a data set that could be summarized based on precipitation state. Median Hg^{II} dry, median Hg^{II} wet, and the median dry-median wet difference for each AMNet site are shown in Fig. 4a–c, respectively, and for Hg^0, these values are plotted in Fig. 4d. Hg^{II} washout ranged from 1–10 pg m^{-3} with an all-site mean of 4 pg m^{-3} (Table 3). Hg^0 enhancement ranged from −0.037 to 0.120 ng m^{-3} with an all-site mean of 0.049 ng m^{-3}, which was notably similar to that observed at the two DCS sites. We hypothesize that the pattern in Hg^0 is related to emissions of Hg^0 from surfaces when they become wet.[58–61]

The washout amount and the percent removal varied by Hg form with GOM percent removal being greater for 15 of 16 sites (all-site mean 81%) than PBM (Table 3). This is consistent with Hg^{II} being the more scavenge-able form. From the Hg^{II} washout pattern across sites shown in Fig. 4c, there is greater Hg^{II} washout for sites that are the Local Emissions category of site

types and also have higher ambient Hg^{II} concentrations (Appendix A, Table 4). The mean Hg^{II} washout amount for Local Emission site group is 6 pg m^{-3}, compared to 2 pg m^{-3} for the two Rural North sites.

Relationships between AMNet atmospheric Hg concentration and $[Hg]_{aq}$ in a weekly precipitation sample are presented in Fig. 5. Each Hg^{II} vs. $[Hg]_{aq}$ data pair represents the weekly averaged GOM + PBM (both wet and dry) and the weekly Hg concentration in the wet deposition sample. In Fig. 5a the mean of weekly average Hg^{II} concentration is weakly linearly correlated to median $[Hg]_{aq}$ across all sites ($r^2 = 0.2$, $p = 0.05$). AL19 and UT97 have the highest Hg^{II} and $[Hg]_{aq}$ concentrations, whereas NS01 and VT99 have the lowest. IN21 and NY43 are positively shifted above the trend, perhaps due to the larger proportion of PBM as Hg^{II} that was observed at these two sites, since PBM is less easily scavenged by precipitation compared to GOM.[41] In contrast the Suburban South group had low Hg^{II} concentrations and elevated $[Hg]_{aq}$ consistent with convective storms that scavenge high altitude RM in the SE U.S. region[29,31] and possibly greater levels of instrument bias due to the humidity.[62,63] The linear trend shown in Fig. 5b for all weekly average Hg^{II} vs. $[Hg]_{aq}$ data for the six Local Emissions sites grouped together is significant ($r^2 = 0.04$, $p < 0.05$), albeit weak, but one must remember that a stronger correlation would probably be seen if it were not for the negative bias in the Hg^{II}
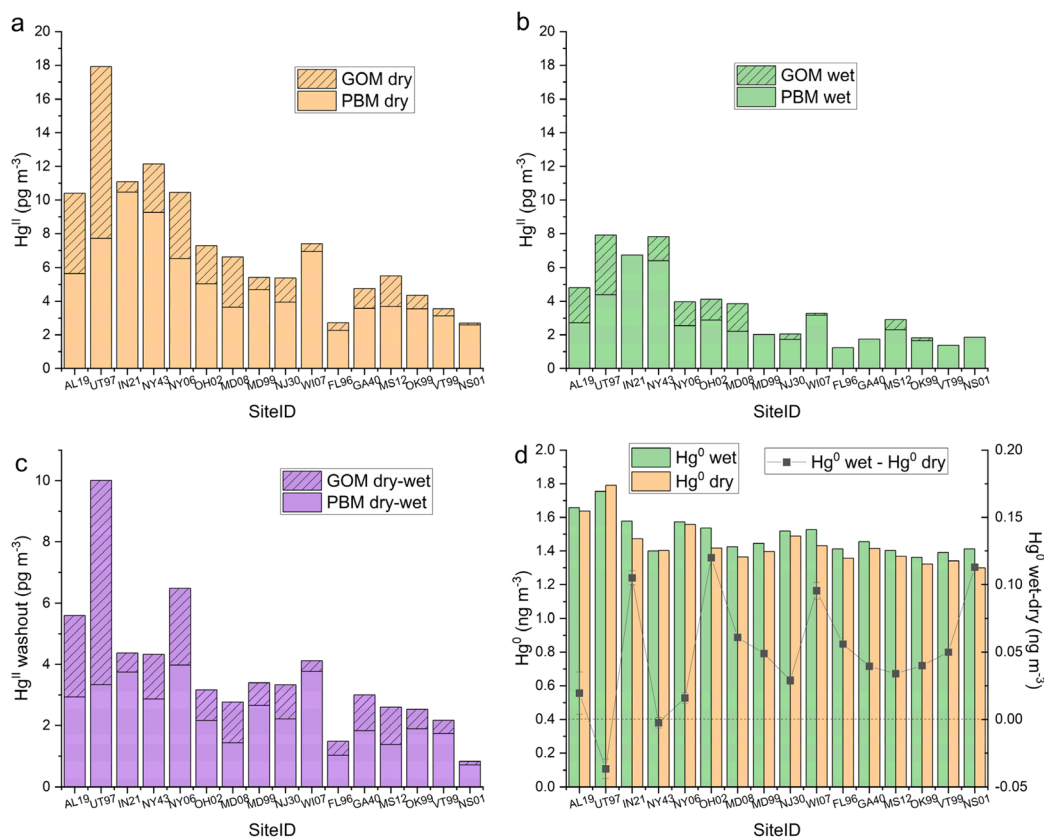

Fig. 4 Comparison of median Hg^{II} concentrations, which is composed of GOM and PBM, at the 16 AMNet sites segregated by precipitation state: (a) dry, (b) wet, (c) the difference between median dry and median wet, and (d) median wet, median dry and wet-dry Hg^0 concentrations. The total height of the bars in panels (a)–(c) represents GOM + PBM = Hg^{II}. The sites are ordered from left to right on the x-axes by site group (Local Emissions, Suburban North, Suburban South, and Rural North).

© 2025 The Author(s). Published by the Royal Society of Chemistry

Environ. Sci.: Atmos., 2025, **5**, 204–219 | **211**

Table 3 Ambient Hg^{II}, median dry-median wet Hg^{II}, Hg^{II} correction estimates, ambient Hg^0 and wet-dry Hg^0 summary data from 16 AMNet sites and 2 sites that used the dual channel system (DCS) method for quantifying Hg^{II}. At the AMNet sites, GOM + PBM = Hg^{II}. Bold text represents mean values for each region of AMNet, for all AMNet, and for the sites with DCS measurements. Data for the AMNet site MD99 are from 2009–2014 for the DCS site MD99 the data are from 2022–2024

Site ID	Median Hg^{II} ambient Hg^{II} pg^{-3}	Median dry-median wet Hg^{II} "washout"			% washout GOM vs. PBM		Correction estimate		Median Hg^0 ambient Hg^0 ng m^{-3}	Median wet-dry Hg^0 enhance Hg^0 ng^{-3}	% increase Hg^0
		PBM pg^{-3}	GOM pg^{-3}	Hg^{II} pg^{-3}	PBM	GOM	Ambient Hg^{II}/ washout Hg^{II}	Hg^{II} corr fact			
AL19	10	3	3	6	55	59	1.8	2.8	1.810	0.020	1.1
UT97	17	3	7	10	44	68	1.7	2.8	1.886	−0.037	−1.9
IN21	11	4	1	4	37	114	2.5	2.0	1.508	0.105	7.0
NY43	12	3	1	4	32	53	2.7	1.8	1.436	−0.003	−0.2
NY06	10	4	3	6	64	68	1.5	3.2	1.684	0.016	1.0
OH02	7	2	1	3	45	48	2.2	2.3	1.453	0.120	8.3
Loc. Emis.	**11**	**3**	**2**	**6**	**46**	**68**	**2.1**	**2.5**	**1.629**	**0.037**	**2.5**
MD08	6	1	1	3	44	48	2.2	2.2	1.360	0.061	4.5
MD99	5	3	1	3	59	119	1.5	3.2	1.400	0.049	3.5
NJ30	5	2	1	3	60	84	1.5	3.2	1.490	0.029	1.9
WI07	7	4	0	4	63	60	1.6	3.1	1.440	0.096	6.6
Sub. North	**7**	**3**	**1**	**3**	**56**	**78**	**1.7**	**2.9**	**1.423**	**0.059**	**4.1**
FL96	3	1	0	1	45	73	2.0	2.5	1.370	0.056	4.1
GA40	5	2	1	3	51	91	1.6	3.0	1.380	0.040	2.9
MS12	4	1	1	3	51	98	1.5	3.2	1.360	0.034	2.5
OK99	4	2	1	3	55	84	1.7	2.9	1.320	0.040	3.0
Sub. South	**5**	**2**	**1**	**2**	**50**	**87**	**1.7**	**2.9**	**1.358**	**0.042**	**3.1**
VT99	4	2	0	2	55	117	1.6	3.0	1.350	0.050	3.7
NS01	3	1	0	1	29	115	3.1	1.6	1.310	0.113	8.6
Rur. North	**4**	**1**	**0**	**2**	**42**	**116**	**2.4**	**2.3**	**1.330**	**0.082**	**6.2**
All AMNet	**7**	**2**	**1**	**4**	**49**	**81**	**1.8**	**2.7**	**1.472**	**0.049**	**3.5**
MD99	43	—	—	7	—	—	5.8	—	—	0.049	3.9
SPL	90	—	—	22	—	—	4.1	—	1.290	0.052	4.2
DCS sites	**66**	—	—	**15**	—	—	**4.9**	—	**1.270**	**0.051**	**4.0**

212 | *Environ. Sci.: Atmos.*, 2025, **5**, 204–219

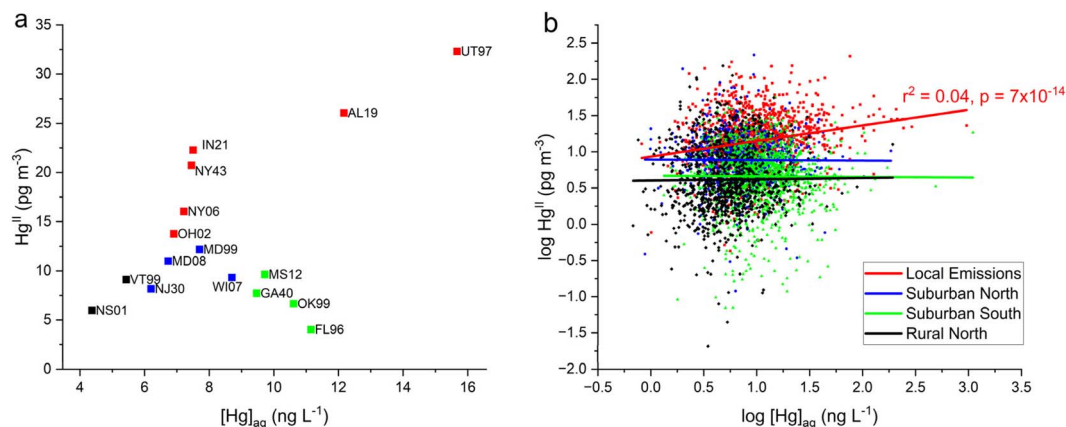© 2025 The Author(s). Published by the Royal Society of Chemistry

Fig. 5 Comparison of AMNet and MDN data for the 16 co-located sites grouped into 4 site types. (a) Mean of Hg^{II} weekly averages (not segregated by precipitation state) *vs.* median $[Hg]_{aq}$ by site. (b) Log of mean of weekly Hg^{II} (GOM + PBM) concentrations *vs.* log of weekly $[Hg]_{aq}$ at. Linear regression statistics in (b) are shown for the data from Local Emissions sites; the other fits shown were not significantly different from zero.

measurements. Uncorrected AMNet Hg^{II} measurements are likely underestimating the contribution from local emissions to wet deposition of Hg.

3.4 Ambient Hg^{II} *vs.* washout Hg^{II}

Here we investigate whether Hg^{II} measurements made at two sites with the DCS method could be used to correct the older measurements made with KCl-denuders across the network. To address this, the relationship was explored between the median ambient Hg^{II} concentration and the median dry–median wet Hg^{II} (washout Hg^{II}) concentrations at each site. We tested whether at any given site using the same measurement method, there would be a constant fraction of ambient Hg^{II} scavenged during precipitation, when averaging over at least an annual cycle. Washout Hg^{II} concentrations for each site were calculated using eqn (1) and these values are plotted on the *x*-axis with median ambient Hg^{II} concentration for each site on the *y*-axis in

Fig. 6a for the two DCS sites and in Fig. 6b for the 16 AMNet sites (note the different scales in the *x*- and *y*-axes). Linear fits for each group of sites were forced through zero and the resulting slopes are 4.8 ± 0.9 and 1.8 ± 0.1 for the DCS and AMNet sites, respectively. Standard deviations of the ambient Hg^{II} and the washout Hg^{II} concentrations are included in Fig. 6a to indicate the uncertainty in the slope that is derived from two DCS data points. Despite the low number of DCS sites, the pattern is clear that the slope from these sites is a factor 2.7 higher than for the AMNet sites.

Based on the observations, it is expected then, that if all the instruments were behaving similarly the ratio of long term median ambient Hg^{II} to washout Hg^{II} concentration should be the same for all the instruments. Using this assumption allows for a potential correction factor which was derived for each AMNet site by using eqn (3) and dividing the Hg^{II} ambient/Hg^{II} washout ratio for the reference sites (DCS) by the same ratio for the AMNet site. This produces site-specific correction factors between 2–3 for each of
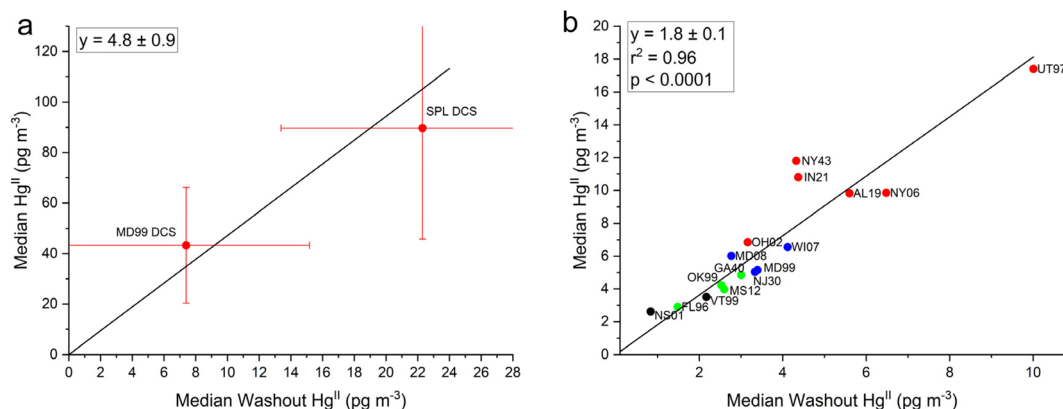

Fig. 6 Median ambient Hg^{II} concentrations plotted against median dry-wet Hg^{II} concentrations for (a) the two dual-channel system (DCS) sites and (b) the 16 AMNet sites color coded by site type (see Fig. 5). The slopes are forced through zero and the error bars in (a) represent the standard deviation of all measurements in the *y*-direction and the standard deviation propagated from error in the dry and wet measurements in the *x*-direction.

Table 4 Summary statistics for hourly air and aqueous Hg concentrations at the co-located MDN and AMNet sites. Oxidized Hg (Hg^{II}) represents PBM + GOM. Site group codes are: LE = Local Emissions, SN = Suburban North, SS = Suburban South, and RN = Rural North.

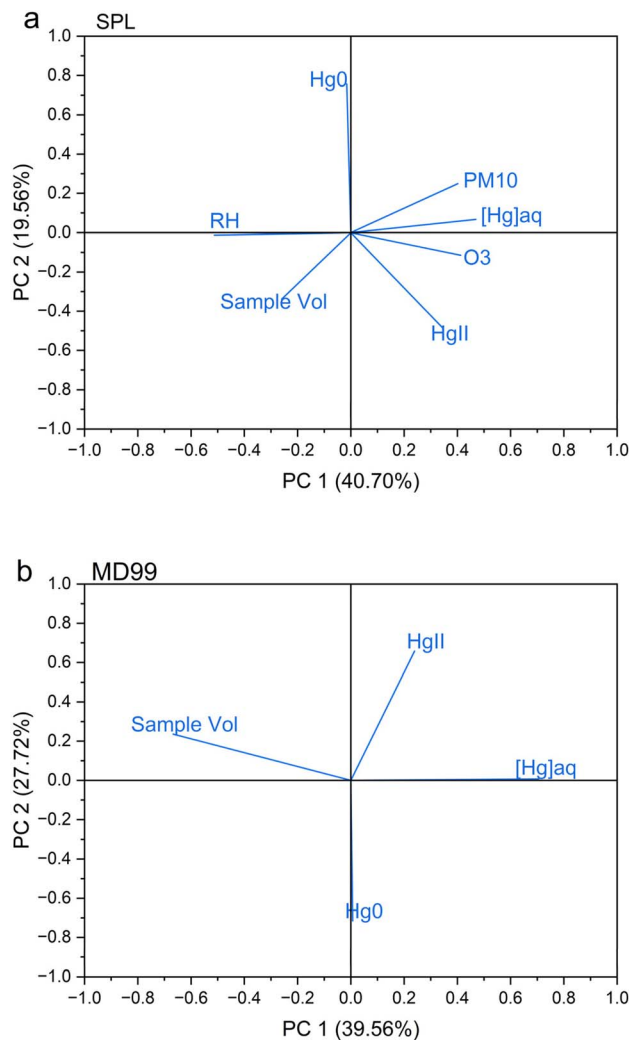| Site ID	Site group	Date range (m/d/y)	Weekly total precip. median mm	Hg conc. median ng L^{-1}	Hg conc. std dev. ng L^{-1}	PBM median pg m^{-3}	PBM std dev. pg m^{-3}	GOM median pg m^{-3}	GOM std dev. pg m^{-3}	Hg^{II} median pg m^{-3}	Hg^{II} std dev. pg m^{-3}	Hg^0 median ng m^{-3}	Hg^0 std dev. ng m^{-3}
AL19	LE	4/11/12–12/16/15	75.3	12.2	19.1	5	34	5	90	10	125	1.810	2.310
UT97	LE	12/2/08–9/27/16	30.7	15.7	66.1	8	45	10	28	17	73	1.886	0.860
IN21	LE	5/3/16–12/31/19	240.1	7.5	10.2	10	39	1	4	11	44	1.508	0.350
NY43	LE	9/30/08–2/2/16	144.2	7.5	7.1	9	19	3	11	12	31	1.436	0.380
NY06	LE	9/2/08–2/2/16	195.4	7.2	6.8	6	18	4	13	10	32	1.684	0.410
OH02	LE	1/16/09–2/26/20	173.6	6.9	7.1	5	16	2	12	7	27	1.453	0.230
MD08	SN	1/6/09–1/2/19	160	6.7	6.8	3	5	3	13	6	17	1.360	0.210
MD99	SN	1/6/09–7/15/14	159.2	7.7	11.1	5	72	1	46	5	118	1.400	0.260
NJ30	SN	10/18/16–8/18/20	213.9	6.2	9.5	4	7	1	5	5	12	1.490	0.280
WI07	SN	7/25/14–12/22/15	95.7	8.7	6.8	6	10	1	4	7	13	1.440	0.240
FL96	SS	12/28/10–12/29/15	106.2	11.2	11.2	2	4	1	4	3	8	1.370	0.170
GA40	SS	1/2/09–12/29/15	72.2	9.5	46.9	4	9	1	7	5	16	1.380	0.260
MS12	SS	3/9/10–3/30/20	189.6	9.7	10.2	3	12	1	8	4	20	1.360	0.180
OK99	SS	1/20/09–5/26/15	136.5	10.6	24.2	3	4	1	4	4	8	1.320	0.210
VT99	RN	1/3/09–12/29/15	143.5	5.4	6.5	3	16	0	4	4	20	1.350	0.220
NS01	RN	1/27/09–11/20/18	238.7	4.4	9.2	3	9	0	2	3	11	1.310	0.230

Fig. 7 Principal component analysis of hourly data collected at the two DCS measurement sites (a) SPL, and (b) MD99, averaged over the hours of measurable precipitation during a weekly MDN sample.

the AMNet sites (Table 3). Prior work to address the low bias in AMNet GOM measurements using a scavenging ratio approach showed that the mean low bias across nine AMNet sites is factor of 2.3,[42] a similar result obtained with the method shown here, suggesting a possible consensus in the directions and magnitude of the correction needed. While the results of this and the Cheng and Zhang[42] studies produced similar results, the benefit of the washout approach described here is that it does not rely upon the assumption that there is a strong empirical relationship between atmospheric oxidized mercury and mercury wet deposition, as was previously assumed.[42]

The washout approach described here assumes a mass balance of Hg^{II} around the sampling site and it must be noted that other processes may be occurring that give rise to uncertainties in this method. These include *in situ* Hg redox reactions and transport of air enriched or depleted in Hg^{II}, especially when these processes might be different under wet and dry conditions. Future measurements and modeling should focus on the response of Hg^{II} and Hg^0 concentrations around the
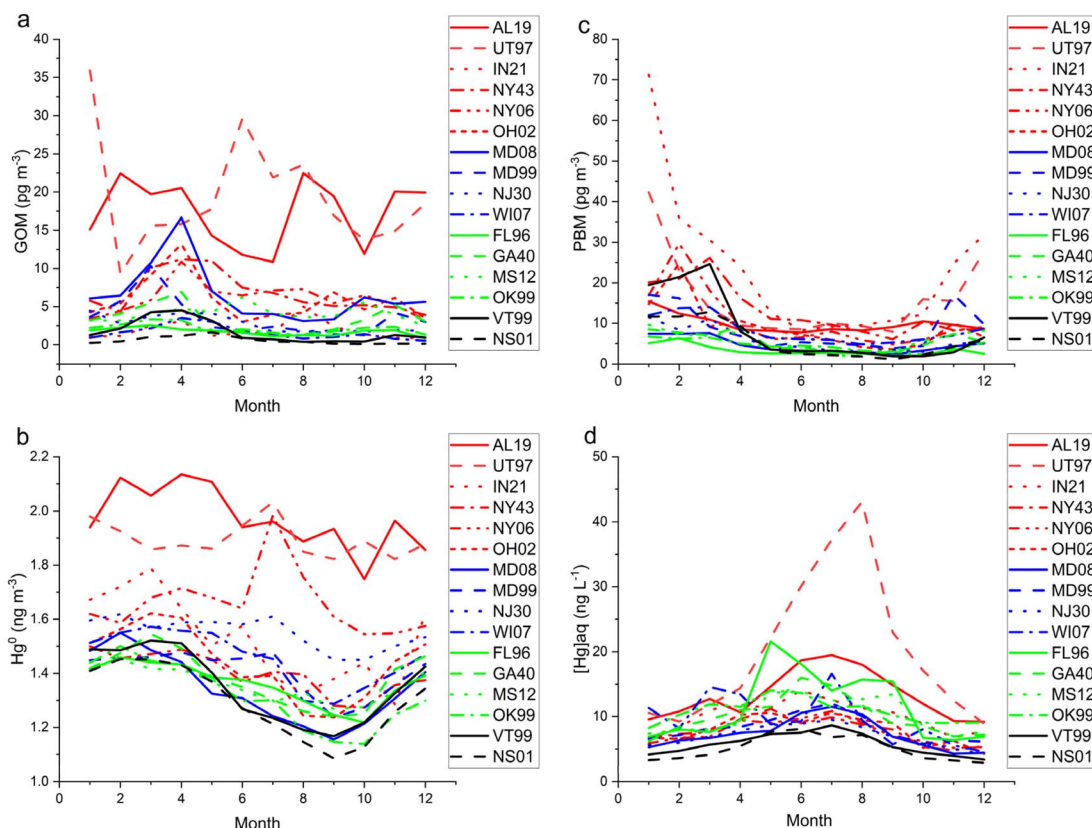
Fig. 8 Mean monthly (a) GOM, (b) PBM, (c) GEM, and (d) median monthly [Hg]$_{aq}$ for the 16 AMNet and MDN sites color-grouped by site type (red = Local Emissions, blue = Suburban North, green = Suburban South, and black = Rural North).
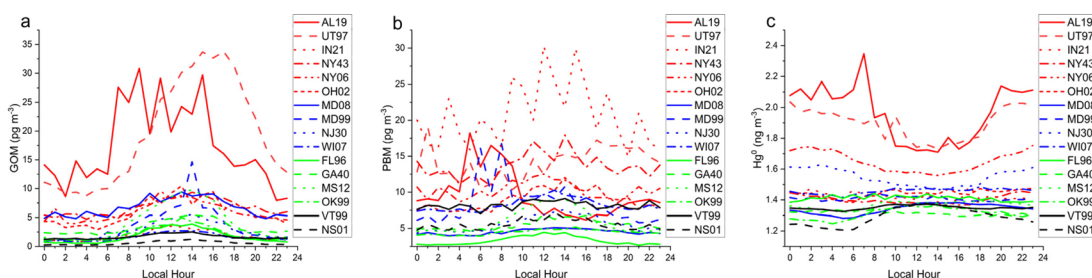

Fig. 9 Mean hourly averages of (a) GOM, (b) PBM, and (c) GEM for the 16 AMNet sites color-grouped by site type, see caption for Fig. 1.

sampling site during dry and wet periods to understand how certain this mass balance approach could be.

4 Conclusions

This study analyzed the behavior of atmospheric Hg as measured with two methods in relation to the effects of precipitation. Two sites made long-term measurements with a dual-channel system for quantifying atmospheric Hg^{II} (SPL and MD99), and these data were used as a basis for comparison of Hg^{II} washout, defined as median [Hg^{II}]$_{dry}$–median [Hg^{II}]$_{wet}$, with older GOM, PBM, and Hg^0 data from 16 co-located sites in the AMNet and MDN networks (also with long-term data) as part of the National Atmospheric

Deposition Program. A reduction in Hg^{II} concentrations during times of precipitation compared to dry conditions (*i.e.* Hg^{II} washout) was observed at all sites regardless of the measurement method, indicating this is a robust feature of the atmosphere due to the effects of precipitation. Similarly, Hg^0 concentrations were higher during times of precipitation at nearly all sites (15 of 17) and likely is related to emissions of Hg^0 from surfaces when they become wet. Measurements with the dual-channel system showed that on average, ambient Hg^{II} concentrations were related to the magnitude of Hg^{II} washout at a given site, with the ratios for SPL and MD99 (the dual-channel system sites) being 4.1 and 5.8, respectively. These relatively similar ratios between DCS sites were observed even though SPL had ambient Hg^{II} concentrations that were 2.1

times higher than MD99. When the same median ambient Hg^{II}/median washout Hg^{II} ratio was calculated for the 16 AMNet sites, it was found that the average ratio for the DCS sites was 2.7 times larger than the average for the AMNet sites. If it is assumed that the ratios from the same type of measurement method should be roughly similar, then it is possible to derive a correction factor using DCS data from a limited number of sites to apply to the AMNet sites. Site-specific correction factors were calculated between 2–3, which compared similarly with factors derived using a scavenging ratio approach[42] giving another potential solution to improving the accuracy of semi quantitative older data.

Correcting older Hg^{II} data is particularly important because a relationship was found between Hg^{II} in the air and $[Hg]_{aq}$ in wet deposition, and thus the proportion of local emissions scavenged from the atmosphere and wet deposited would be underestimated if the currently available measurements were used to calculate a flux. Furthermore, uncorrected observations are often used to validate chemical models; therefore, to improve source attribution studies and global model validity, it is critical to improve the accuracy of the available data even if the correction method itself is an estimate. Future work should make at least one-year worth of measurements using the DCS at multiple AMNet sites to calculate Hg^{II} washout and compare with ambient Hg^{II} concentrations in order verify if the correction factors suggested here still agree.

Data availability

The raw data from Storm Peak Laboratory are publicly available from at **https://doi.org/10.5281/zenodo.10699270**. The data from Beltsville, MD are also publicly available and can be obtained by sending an email to Winston.luke@noaa.gov. The AMNet and MDN data are publicly available through the NADP website **https://nadp.slh.wisc.edu/**.

Author contributions

Peter Weiss-Penzias – conceptualization, investigation, data compilation and analysis, supervision, and lead writing of original draft and the final manuscript. Seth Lyman – collection of measurement data, design, construction, and testing of dual channel instrument, contributor to writing of the original draft and the final manuscript. Tyler Elgiar – collection of measurement data, construction, and testing of dual channel instrument. Lynne Gratz – collection of measurement data, contributor to writing of the original draft and the final manuscript. Winston Luke – collection of measurement data, construction, and testing of dual channel instrument. Gabriel Quevedo – data compilation and analysis. Nicole Choma – data compilation. Mae S. Gustin – conceptualization, resources, supervision, contributor to writing of original draft and the final manuscript.

Conflicts of interest

There are no conflicts of interest to declare.

Appendices

Appendix A: seasonal and diel cycles of AMNet-MDN Hg data

A list of the 16 co-located sites considered in this study, their measurement periods, and summary statistics for Hg are shown in Appendix Table 4. Medians were calculated for $[Hg]_{aq}$ to minimize the effect of single high sample since $N = 4$ or fewer for each month. The mean monthly concentrations of PBM, GOM, and Hg^0 from AMNet sites, and the median monthly concentrations of $[Hg]_{aq}$ from the co-located MDN sites are shown in Fig. 7. Fig. 8 shows the mean hourly concentrations of PBM, GOM, and Hg^0 from AMNet sites. Among the 16 sites, PBM concentrations were >75th percentile compared to all sites data at NY06, NY43, IN21, and UT97, GOM concentrations were >75th percentile at AL19, MD08, NY43, and UT97, and Hg^0 concentrations were >75th percentile at AL19, NJ30, NY06, and UT97. Most sites showed a springtime maximum for GOM, a wintertime maximum for PBM, an early springtime maximum for Hg^0, and a summertime maximum for $[Hg]_{aq}$ (Fig. 7). Across all sites, the magnitude of the seasonal cycle for Hg^0 was in the 0.2–0.4 ng m^{-3} range, and GOM and PBM varied by 2–60 pg m^{-3}, although these data are biased low, and the magnitude of the bias is dependent on which Hg^{II} forms are present and the ambient atmospheric chemistry. Trends such as these could also be due to trends in underlying non-Hg chemistry that impacts KCl-denuder performance, rather than due to trends in GOM itself. Concentrations of Hg in wet deposition displayed a warm-season maximum at all sites[32] with UT97 displaying the highest summertime concentrations, probably due to its arid climate and low sample volume.[23]

The diel cycles of GOM demonstrated that it is a daytime form at least in the boundary layer, reaching a maximum at nearly every site in the afternoon (Fig. 8). AL19 is known to be impacted by local sources of GOM[64] and thus displayed an earlier-shifted maximum compared to the other sites, reflecting the daily breakup of the nocturnal boundary layer.[65] The diel pattern at UT97 is of similar magnitude as AL19, consistent with industrial sources in its vicinity,[66] but is shifted later and smoother, indicating photochemistry or deep convective mixing is more important at this site. The PBM diel pattern is noisier than that for GOM, but generally shows a daytime increase in concentrations, for example at OH02 the amplitude of the cycle is 5 pg m^{-3} with a peak at 14:00 local time. Nocturnal boundary layer trapping of pollutants is evident in the diel pattern of PBM at AL19 with a peak in concentrations at 04:00 local time. IN21 displayed the highest PBM concentrations of any site; the small number of samples and the 3 hours measurement cycle produced the sawtooth pattern in Fig. 8. Hg^0 diel patterns show a daytime minimum for the more polluted sites which could reflect a combination of plant uptake and the mixing of cleaner air from aloft throughout the day, and a daytime maxima or no diel pattern for the more background sites. Looking across all sites, the magnitude of the diel cycle for Hg^0 is in the 0.1–0.2 ng m^{-3} range, and GOM and PBM vary by 2–20 pg m^{-3} although, as stated before, these data are biased low.

Acknowledgements

References

1 T. W. Clarkson, Environmental contaminants in the food chain, *Am. J. Clin. Nutr.*, 1995, **61**, 682S–686S.

2 D. Mergler, H. A. Anderson, L. H. Chan, *et al.*, Methylmercury exposure and health effects in humans: a worldwide concern, *Ambio*, 2007, **36**, 3–11.

3 C. A. Eagles-Smith, J. J. Willacker, S. J. Nelson, *et al.*, A National-Scale Assessment of Mercury Bioaccumulation in United States National Parks Using Dragonfly Larvae As Biosentinels through a Citizen-Science Framework, *Environ. Sci. Technol.*, 2020, **54**, 8779–8790.

4 P. A. Ariya, M. Amyot, A. Dastoor, *et al.*, Mercury physicochemical and biogeochemical transformation in the atmosphere and at atmospheric interfaces: a review and future direction, *Chem. Rev.*, 2015, **115**, 3760–3802.

5 A. Saiz-Lopez, S. P. Sitkiewicz, D. Roca-Sanjuán, *et al.*, Photoreduction of gaseous oxidized mercury changes global atmospheric mercury speciation, transport and deposition, *Nat. Commun.*, 2018, **9**, 4796.

6 X. Yang, M. Jiskra and J. E. Sonke, Experimental rainwater divalent mercury speciation and photoreduction rates in the presence of halides and organic carbon, *Sci. Total Environ.*, 2019, **697**, 133821.

7 V. Shah, D. J. Jacob, C. P. Thackray, *et al.*, Improved Mechanistic Model of the Atmospheric Redox Chemistry of Mercury, *Environ. Sci. Technol.*, 2021, **55**, 14445–14456.

8 A. Saiz-Lopez, O. Travnikov, J. E. Sonke, *et al.*, Photochemistry of oxidized Hg(I) and Hg(II) species suggests missing mercury oxidation in the troposphere, *Proc. Natl. Acad. Sci. U. S. A.*, 2020, **117**, 30949–30956.

9 S. N. Lyman, T. Elgiar, M. S. Gustin, S. M. Dunham-Cheatham, L. M. David and L. Zhang, Evidence against Rapid Mercury Oxidation in Photochemical Smog, *Environ. Sci. Technol.*, 2022, **56**, 11225–11235.

10 S. N. Lyman, I. Cheng, L. E. Gratz, P. Weiss-Penzias and L. Zhang, An updated review of atmospheric mercury, *Sci. Total Environ.*, 2020, **707**, 135575.

11 J. Zhou and D. Obrist, Global Mercury Assimilation by Vegetation, *Environ. Sci. Technol.*, 2021, **55**, 14245–14257.

12 L. Zhang, P. Blanchard, D. A. Gay, E. Prestbo, M. Risch, D. Johnson, J. Narayan, R. Zsolway, T. Holsen and E. Miller, Estimation of speciated and total mercury dry deposition at monitoring locations in eastern and central North America, *Atmos. Chem. Phys.*, 2012, **12**, 4327–4340.

13 D. O'Connor, D. Hou, Y. S. Ok, *et al.*, Mercury speciation, transformation, and transportation in soils, atmospheric flux, and implications for risk management: A critical review, *Environ. Int.*, 2019, **126**, 747–761.

14 J. Munthe, R. A. Bodaly, B. A. Branfireun, *et al.*, Recovery of mercury-contaminated fisheries, *Ambio*, 2007, **36**, 33–44.

15 C. A. Eagles-Smith, J. T. Ackerman, J. J. Willacker, *et al.*, Spatial and temporal patterns of mercury concentrations in freshwater fish across the Western United States and Canada, *Sci. Total Environ.*, 2016, **568**, 1171–1184.

16 R. Ferrara, B. Maserti, A. Petrosino and R. Bargagli, Mercury levels in rain and air and the subsequent washout mechanism in a central Italian region, *Atmos. Environ.*, 1986, **1967**, 125–128.

17 G. E. Glass, J. A. Sorensen, K. W. Schmidt, G. R. Rapp, D. Yap and D. Fraser, Mercury deposition and sources for the upper Great Lakes region, *Water, Air, Soil Pollut.*, 1991, **56**, 235–249.

18 J. Huang, M. B. Miller, P. Weiss-Penzias and M. S. Gustin, Comparison of gaseous oxidized Hg measured by KCl-coated denuders, and nylon and cation exchange membranes, *Environ. Sci. Technol.*, 2013, **47**, 7307–7316.

19 C. D. McClure, D. A. Jaffe and E. S. Edgerton, Evaluation of the KCl denuder method for gaseous oxidized mercury using $HgBr_2$ at an in-service AMNet site, *Environ. Sci. Technol.*, 2014, **48**, 11437–11444.

20 M. S. Landis, A. F. Vette and G. J. Keeler, Atmospheric mercury in the Lake Michigan basin: influence of the Chicago/Gary urban area, *Environ. Sci. Technol.*, 2002, **36**, 4508–4517.

21 E. M. White, M. S. Landis, G. J. Keeler and J. A. Barres, Investigation of mercury wet deposition physicochemistry in the Ohio River Valley through automated sequential sampling, *Sci. Total Environ.*, 2013, **448**, 107–119.

22 L. E. Gratz, G. J. Keeler and E. K. Miller, Long-term relationships between mercury wet deposition and meteorology, *Atmos. Environ.*, 2009, **43**, 6218–6229.

23 P. S. Weiss-Penzias, D. A. Gay, M. E. Brigham, M. T. Parsons, M. S. Gustin and A. Ter Schure, Trends in mercury wet deposition and mercury air concentrations across the U.S. and Canada, *Sci. Total Environ.*, 2016, **568**, 546–556.

24 Y. M. Wang, D. Y. Wang, B. Meng, Y. L. Peng, L. Zhao and J. S. Zhu, Spatial and temporal distributions of total and methyl mercury in precipitation in core urban areas, Chongqing, China, *Atmos. Chem. Phys.*, 2012, **12**, 9417–9426.

25 Z. Ye, H. Mao and C. T. Driscoll, Primary effects of changes in meteorology vs. anthropogenic emissions on mercury wet deposition: a modeling study, *Atmos. Environ.*, 2019, **198**, 215–225.

26 C. Pearson, D. Howard, C. Moore and D. Obrist, Mercury and trace metal wet deposition across five stations in Alaska: controlling factors, spatial patterns, and source regions, *Atmos. Chem. Phys.*, 2019, **19**, 6913–6929.

27 X. Nie, C. Wu, H. Zhang, Y. Li, T. Li and Y. Wang, Atmospheric wet deposition of mercury in urban Jinan, eastern China: Speciation, scavenging process and

© 2025 The Author(s). Published by the Royal Society of Chemistry

Environ. Sci.: Atmos., 2025, **5**, 204–219 | 217

potential sources, *Ecotoxicol. Environ. Saf.*, 2023, **251**, 114529.

28 H. Zhou, C. Zhou, P. K. Hopke and T. M. Holsen, Mercury wet deposition and speciated mercury air concentrations at rural and urban sites across New York state: Temporal patterns, sources and scavenging coefficients, *Sci. Total Environ.*, 2018, **637–638**, 943–953.

29 V. Shah and L. Jaeglé, Subtropical subsidence and surface deposition of oxidized mercury produced in the free troposphere, *Atmos. Chem. Phys.*, 2017, **17**, 8999–9017.

30 J. Huang and M. S. Gustin, Evidence for a free troposphere source of mercury in wet deposition in the Western United States, *Environ. Sci. Technol.*, 2012, **46**, 6621–6629.

31 A. S. Kaulfus, U. Nair, C. D. Holmes and W. M. Landing, Mercury Wet Scavenging and deposition differences by precipitation type, *Environ. Sci. Technol.*, 2017, **51**, 2628–2634.

32 E. M. Prestbo and D. A. Gay, Wet deposition of mercury in the US and Canada, 1996–2005: Results and analysis of the NADP mercury deposition network (MDN), *Atmos. Environ.*, 2009, **43**, 4223–4233.

33 D. A. Jaffe, S. Lyman, H. Amos, M. S. Gustin, J. Huang, N. E. Selin, L. Levin, A. Ter Schure, R. P. Mason, R. Talbot, A. Rutter, *et al.*, Progress on understanding atmospheric mercury hampered by uncertain measurements, *Environ. Sci. Technol.*, 2014, **48**, 7204–7206.

34 S. N. Lyman, D. A. Jaffe and M. S. Gustin, Release of mercury halides from KCl denuders in the presence of ozone, *Atmos. Chem. Phys.*, 2010, **10**, 8197–8204.

35 N. Allen, J. Gacnik, S. M. Dunham-Cheatham and M. S. Gustin, Tests of alternate membranes and alternate configurations for the Reactive Mercury Active System, *Atmos. Environ.*, 2024, **318**, 120240.

36 A. Luippold, M. S. Gustin, S. M. Dunham-Cheatham and L. Zhang, Improvement of quantification and identification of atmospheric reactive mercury, *Atmos. Environ.*, 2020, **224**, 117307.

37 S. N. Lyman, L. E. Gratz, S. M. Dunham-Cheatham, M. S. Gustin and A. Luippold, Improvements to the Accuracy of Atmospheric Oxidized Mercury Measurements, *Environ. Sci. Technol.*, 2020, **54**, 13379–13388.

38 X. Bu, H. Zhang, G. Lv, H. Lin, L. Chen, X. Yin, *et al.*, Comparison of reactive gaseous mercury collection by different sampling methods in a laboratory test and field monitoring, *Environ. Sci. Technol. Lett.*, 2018, **5**, 600–607.

39 Y. Tang, S. Wang, G. Li, *et al.*, Elevated Gaseous Oxidized Mercury Revealed by a Newly Developed Speciated Atmospheric Mercury Monitoring System, *Environ. Sci. Technol.*, 2022, **56**, 7707–7715.

40 S. Chen, X. Qiu, L. Zhang, F. Yang and P. Blanchard, Method development estimating ambient oxidized mercury concentration from monitored mercury wet deposition, *Atmos. Chem. Phys.*, 2013, **13**, 11287–11293.

41 I. Cheng, L. Zhang and H. Mao, Relative contributions of gaseous oxidized mercury and fine and coarse particle-bound mercury to mercury wet deposition at nine

monitoring sites in North America, *J. Geophys. Res. Atmos.*, 2015, **120**, 8549–8562.

42 I. Cheng and L. Zhang, Uncertainty Assessment of Gaseous Oxidized Mercury Measurements Collected by Atmospheric Mercury Network, *Environ. Sci. Technol.*, 2017, **51**, 855–862.

43 M. S. Gustin, S. M. Dunham-Cheatham, J. Huang, S. Lindberg and S. N. Lyman, Development of an understanding of reactive mercury in ambient air: A review, *Atmosphere*, 2021, **12**, 73.

44 M. S. Gustin, S. M. Dunham-Cheatham, N. Allen, *et al.*, Observations of the chemistry and concentrations of reactive Hg at locations with different ambient air chemistry, *Sci. Total Environ.*, 2023, **904**, 166184.

45 M. M. Lynam, J. T. Dvonch, J. A. Barres, M. S. Landis and A. S. Kamal, Investigating the impact of local urban sources on total atmospheric mercury wet deposition in Cleveland, Ohio, USA, *Atmos. Environ.*, 2016, **127**, 262–271.

46 M. Muntean, G. Janssens-Maenhout, S. Song, A. Giang, N. E. Selin and H. Zhong, *et. al.*, Evaluating EDGARv4. tox2 speciated mercury emissions ex-post scenarios and their impacts on modelled global and regional wet deposition patterns, *Atmos. Environ.*, 2018, **184**, 56–68.

47 X. Faïn, D. Obrist, A. G. Hallar, I. Mccubbin and T. Rahn, High levels of reactive gaseous mercury observed at a high elevation research laboratory in the Rocky Mountains, *Atmos. Chem. Phys.*, 2009, **9**, 8049–8060.

48 D. Obrist, A. G. Hallar, I. McCubbin, B. B. Stephens and T. Rahn, Atmospheric mercury concentrations at Storm Peak Laboratory in the Rocky Mountains: Evidence for long-range transport from Asia, boundary layer contributions, and plant mercury uptake, *Atmos. Environ.*, 2008, **42**, 7579–7589.

49 T. R. Elgiar, S. N. Lyman, T. D. Andron, L. Gratz, A. G. Hallar, M. Horvat, S. Vijayakumaran, T. O'Neil, R. Volkamer and I. Živković, Traceable Calibration of Atmospheric Oxidized Mercury Measurements, *Environ. Sci. Technol.*, 2024, **58**, 10706–10716.

50 S. M. Dunham-Cheatham, S. Lyman and M. S. Gustin, Comparison and calibration of methods for ambient reactive mercury quantification, *Sci. Total Environ.*, 2023, **856**, 159219.

51 E. J. Derry, T. R. Elgiar, T. Y. Wilmot, N. W. Hoch, N. S. Hirshorn, P. Weiss-Penzias, C. F. Lee, J. C. Lin, A. G. Hallar, R. Volkamer and S. N. Lyman, Elevated oxidized mercury in the free troposphere: Analytical advances and application at a remote continental mountaintop site, *Atmos. Chem. Phys.*, 2024, **24**, 9615–9643.

52 L. J. Ambrose, Improved methods for signal processing in measurements of mercury by Tekran® 2537A and 2537B instruments, *Atmos. Meas. Tech.*, 2017, **10**, 5063–5073.

53 M. B. Miller, M. S. Gustin and G. C. Edwards, Reactive mercury flux measurements using cation exchange membranes, *Atmos. Meas. Tech. Discuss.*, 2018, **2018**, 1–28.

54 X. Ren, W. T. Luke, P. Kelley, M. D. Cohen, M. L. Olson, J. Walker, R. Cole, M. Archer, R. Artz and A. A. Stein, Long-Term Observations of Atmospheric Speciated Mercury at

a Coastal Site in the Northern Gulf of Mexico during 2007–2018, 2020, *Atmosphere*, **11**, 268.

55 S. M. Dunham-Cheatham, S. Lyman and M. S. Gustin, Evaluation of sorption surface materials for reactive mercury compounds, *Atmos. Environ.*, 2020, **242**, 117836.

56 N. Allen, J. Gačnik, S. M. Dunham-Cheatham and M. S. Gustin, Interaction of reactive mercury with surfaces and implications for atmospheric mercury speciation measurements, *Atmos. Environ.*, 2024, **318**, 120240.

57 X. Lan, R. Talbot, M. Castro, K. Perry and W. Luke, Seasonal and diurnal variations of atmospheric mercury across the US determined from AMNet monitoring data, *Atmos. Chem. Phys.*, 2012, **12**, 10569–10582.

58 X. Song and B. Van Heyst, Volatilization of mercury from soils in response to simulated precipitation, *Atmos. Environ.*, 2005, **39**, 7494–7505.

59 M. S. Gustin, S. E. Lindberg and P. J. Weisberg, An update on the natural sources and sinks of atmospheric mercury, *Appl. Geochem.*, 2008, **23**, 482–493.

60 C. Briggs and M. S. Gustin, Building upon the conceptual model for soil mercury flux: Evidence of a link between moisture evaporation and Hg evasion, *Water, Air, Soil Pollut.*, 2013, **224**, 1744.

61 M. S. Gustin, J. A. Ericksen, D. E. Schorran, D. W. Johnson, S. E. Lindberg and J. S. Coleman, Application of controlled mesocosm for understanding mercury plant-soil-air exchange, *Environ. Sci. Technol.*, 2004, **38**, 6044–6050.

62 J. Huang, M. B. Miller, P. Weiss-Penzias and M. S. Gustin, Comparison of gaseous oxidized Hg measured by KCl-coated denuders, and nylon and cation exchange membranes, *Environ. Sci. Technol.*, 2013, **47**, 7307–7316.

63 S. Lyman, C. Jones, T. O'Neil, *et al.*, Automated Calibration of Atmospheric Oxidized Mercury Measurements, *Environ. Sci. Technol.*, 2016, **50**, 12921–12927.

64 U. S. Nair, Y. Wu, J. Walters, J. Jansen and E. S. Edgerton, Diurnal and seasonal variation of mercury species at coastal-suburban, urban, and rural sites in the southeastern United States, *Atmos. Environ.*, 2012, **47**, 499–508.

65 H. Mao and R. Talbot, Speciated mercury at marine, coastal, and inland sites in New England–Part 1: Temporal variability, *Atmos. Chem. Phys.*, 2012, **12**, 5099–5112.

66 C. Peterson and M. S. Gustin, Mercury in the air, water and biota at the Great Salt Lake (Utah, USA), *Sci. Total Environ.*, 2008, **405**, 255–268.

© 2025 The Author(s). Published by the Royal Society of Chemistry

Environ. Sci.: Atmos., 2025, **5**, 204–219 | **219**